

Topical Review

Kinetic Properties of Ion Carriers and Channels

P. Läuger

Department of Biology, University of Konstanz, D-7750 Konstanz, Germany

Ions and other hydrophilic substances permeate through cellular membranes by means of special mechanisms different from simple diffusion through the lipid bilayer. In the discussion of possible transport pathways, two alternatives are usually considered: carrier and channel mechanisms. A carrier (in its simplest form) may be defined as a transport system with a binding side that is exposed alternately to the left and to the right side (but not to both sides simultaneously). A channel, on the other hand, consists of one or several binding sites arranged in a transmembrane sequence and is accessible from both sides at the same time.

Clear-cut examples of carrier and channel mechanisms in ion transport have been obtained from the study of certain small or medium-sized peptides and depsipeptides produced by microorganisms. Cyclopeptides, such as valinomycin, have been shown to act by a translocatory carrier mechanism which involves a movement of the whole carrier molecule with respect to the lipid matrix of the membrane. A well-characterized ion channel is the channel formed by the linear pentadecapeptide, gramicidin A. In these cases the distinction between a channel which is more or less fixed within the membrane and a carrier moving within the lipid matrix is unambiguous. The discrimination between carrier and channel mechanisms becomes less obvious, however, in the case of large membrane proteins spanning the lipid bilayer, which are thought to be responsible for ion transport across the cell membrane. Such a protein is unlikely to move as a whole within the membrane. It still can act as carrier (according to the definition given above), however, if a conformational change within the protein switches the binding site from a left-exposed to a right-exposed state. A channel, on the other hand, does not necessarily have a fixed, time-independent structure. Proteins may assume many conformational substates and move from one state to the

other. Accordingly, in a channel conformational transitions may occur between states differing in the height of the energy barriers that restrict the movement of the ion. It can be shown that such a channel with multiple conformational states may approach the kinetic behavior of a carrier. Channel and carrier models should therefore not be regarded as mutually exclusive possibilities, but rather as limiting cases of a more general mechanism.

In this article first the kinetic properties of well-studied examples of carriers and channels will be reviewed, namely, translocatory ion carriers of the valinomycin type and ion channels formed by peptides such as gramicidin A. This will be followed by a theoretical treatment of ion movement in channels with fixed structure and a comparison of the transport properties of simple carriers and channels. In the last part of the article, the more general concept of channels with multiple conformational states will be discussed, which allows one to describe carrier and channel mechanisms from a common point of view. The same concept will also be applied to active ion-transport systems (ion pumps) in which the state of the channel is transiently changed by energy uptake from an external source.

Kinetic Analysis of Translocatory Ion Carriers

Incorporation of certain macrocyclic antibiotics, such as valinomycin, enniatin B, and the macrotetrolides into artificial lipid bilayer membranes result in a strong increase of potassium permeability of the membrane [20, 70]. In solution these compounds form complexes with alkali ions in which the primary hydration shell of the ion is replaced by ligand groups from the macrocycle (Fig. 1). All experiments carried out so far are consistent with the notion that valinomycin and related compounds act by a translocatory carrier mechanism. Both the stationary [66,

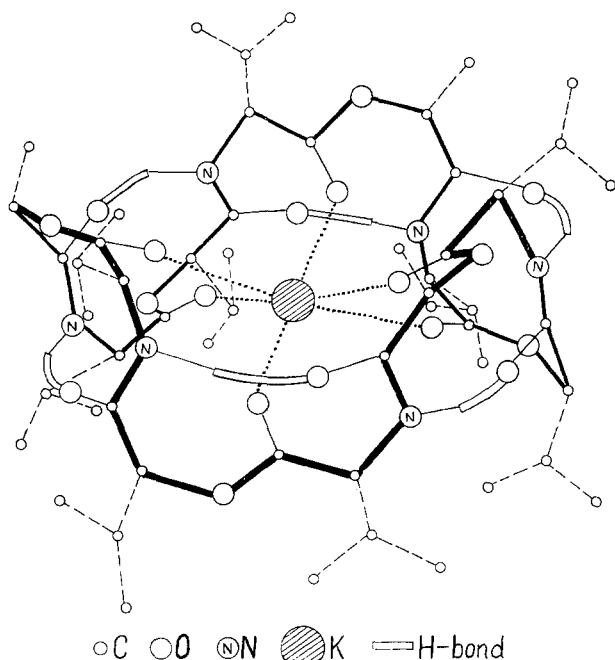


Fig. 1. Structure of the valinomycin- K^+ complex [64]

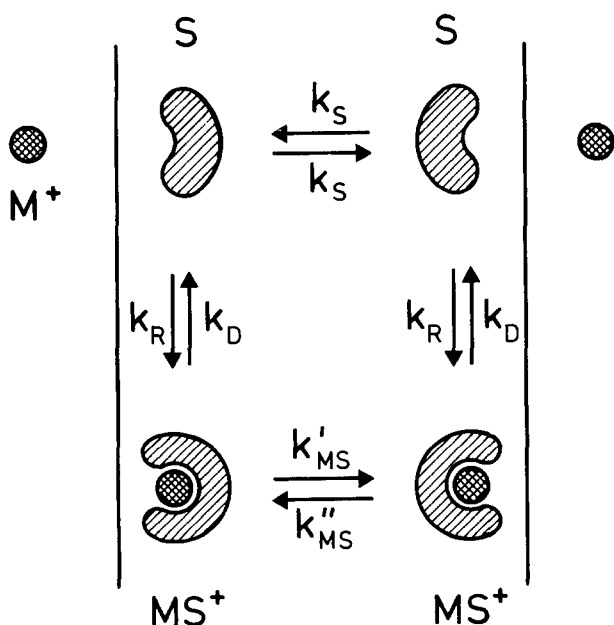


Fig. 2. Transport of ion M^+ mediated by a translocatory carrier S

70] as well as the nonstationary [67] behavior of macrocyclic ion carriers in planar bilayer membranes could be approximately described on the basis of the assumption that the overall transport occurs in four distinct steps (Fig. 2): (i) association of ion M^+ and carrier S in the interface, (ii) translocation of the complex MS^+ , (iii) dissociation of MS^+ , (iv) back transport of free carriers S . In the analysis of the experiments it is further assumed that the individual

reaction steps can be described in the same way as chemical processes, introducing reaction rate constants. These assumptions are only approximately correct. In reality, both the association and dissociation reaction (rate constants k_R and k_D) are multistep processes, involving the stepwise exchange of water molecules and ligand groups, as well as conformational rearrangements of the carrier molecule. k_R and k_D are determined by the rate-limiting steps in the overall process, probably conformational changes of the carriers. The description of the two translocation processes by monomolecular rate constants (k_{MS} and k_S) is a further approximation that may be justified by the expectation that both the free carrier and the complex are located in deep potential energy minima at the membrane-solution interface for most of the time [3, 41, 64].

The kinetics of the ion carrier may be analyzed by studying the electrical conductance of planar bilayer membranes. In particular, electrical relaxation techniques, such as the voltage-jump [67] or charge-pulse method [18] may be used to evaluate the individual rate constants. Such experiments have been carried out in the last years with a number of different carrier systems and membranes of different lipid composition [13–15, 18, 19]. As a specific example, we consider the results obtained for valinomycin/ Rb^+ in a monoolein/*n*-decane membrane (25 °C, 1 M $RbCl$) [18]:

$$k_R \approx 3 \times 10^5 \text{ M}^{-1} \text{ s}^{-1}$$

$$k_D \approx 2 \times 10^5 \text{ s}^{-1}$$

$$k_{MS} \approx 3 \times 10^5 \text{ s}^{-1}$$

$$k_S \approx 4 \times 10^4 \text{ s}^{-1}$$

At one-molar concentration of the transported ion ($c_M = 1 \text{ M}$), the rate constants of association ($c_M k_R$), dissociation (k_D) and translocation of the loaded carrier (k_{MS}) are approximately equal ($2\text{--}3 \times 10^5 \text{ s}^{-1}$). The rate-determining step in this system is the back transport of the free carrier ($k_S \approx 4 \times 10^4 \text{ s}^{-1}$). $k_{MS} \approx 3 \times 10^5 \text{ s}^{-1}$ is the frequency by which the ion-carrier complex crosses the central barrier; the reciprocal value $1/k_{MS} \approx 3 \mu\text{sec}$ is the average time required for translocation. This time may be compared with the diffusion time $\tau = d^2/2D$ of a spherical particle of the size of the carrier across the same distance (membrane thickness $d \approx 5 \text{ nm}$) in water (diffusion coefficient $D \approx 3 \times 10^{-6} \text{ cm}^2 \text{ s}^{-1}$), which is about $0.04 \mu\text{sec}$.

An important quantity for the kinetic description of carriers (and other transport systems) is the maximum turnover rate f . f is defined as the limiting transport rate which is approached under short-circuit conditions for infinite ion concentration on the

Table 1. Rate constants of valinomycin-mediated transport through membranes made from monoglycerides with different fatty acid residues [15]^a

Fatty acid	k_R $10^4 \text{ M}^{-1} \text{ s}^{-1}$	k_D 10^4 s^{-1}	k_{MS} 10^4 s^{-1}	k_S 10^4 s^{-1}
Variation of chain length				
16:1	43	13	74	8.5
18:1	37	24	27	3.5
20:1	23	12	10	1.8
22:1	24	13	7	1.1
Variation of the number of double bonds				
20:1	23	12	10	1.8
20:2	34	9	39	3.2
20:3	34	5	136	9.4
20:4	42	3	240	12

^a Palmitoleoyl (16:1), oleoyl (18:1), Δ^{11} -eicosenoyl (20:1), erucoyl (22:1), $\Delta^{11,14}$ -eicosadienoyl (20:2), $\Delta^{11,14,17}$ -eicosatrienoyl (20:3) and arachidonoyl (20:4). The solvent for membrane formation was *n*-decane; $T=25^\circ\text{C}$.

cis-side and zero ion concentration of the *trans*-side. In the above example, f is about $3 \times 10^4 \text{ s}^{-1}$. The high efficiency of valinomycin as an ion carrier mainly results from this high turnover rate, whereas the binding constant for the ion, $k_R/k_D \approx 1.5 \text{ M}^{-1}$, is rather low.

For a translocatory carrier mechanism the rate constants may be expected to depend on the structure and fluidity of the membrane. Indeed, a strong influence of lipid composition of the membrane on valinomycin-mediated ion transport has been observed [14, 15, 19]. Some results obtained with monoglyceride membranes differing in the number of double bonds and the chain length of the lipid are summarized in Table 1. It is seen that increasing the chain length from C_{16} to C_{22} results in a eight- to tenfold decrease of the translocation rate constants k_S and k_{MS} , whereas k_R and k_D show little variation. Increasing the number of double bonds from one to four increases k_S eightfold and k_{MS} 24-fold. These

variations of k_S and k_{MS} presumably result (at least in part) from the increase of microviscosity with increasing chain length and decreasing number of double bonds. Another effect which may influence k_{MS} is the increase of dielectric constant with increasing unsaturation. Such an increase of dielectric constant would reduce the energy barrier for the translocation of the charged complex.

The Gramicidin Channel as a Model Channel

The finding that gramicidin A, a hydrophobic peptide with known primary structure, forms alkali-ion permeable channels in lipid bilayer membranes [32] opened up the possibility of studying ion permeation through channels in a simple model system. Gramicidin A is a linear pentadecapeptide with the sequence $\text{HCO-L-Val-Gly-L-Ala-D-Leu-L-Ala-D-Leu-L-Val-D-Leu-L-Trp-D-Leu-L-Trp-D-Leu-L-Trp-D-Leu-L-Trp-NHCH}_2\text{CH}_2\text{OH}$. Evidence that gramicidin A forms channels (and does not act as a mobile carrier) has been obtained in experiments in which very small amounts of the peptide were added to a planar bilayer membrane [32]. Under this condition the membrane current under a constant applied voltage fluctuates in a step-like manner (Fig. 3). The size of the single conductance step is about 90 pS in 1 M Cs^+ , corresponding to a transfer of $6 \times 10^7 \text{ Cs}^+$ ions per sec. This transport rate is larger by a factor of about one thousand than the turnover number of a mobile carrier of the valinomycin type (*see above*), making a translocatory carrier mechanism highly unlikely. Further evidence for a channel mechanism comes from the observation that the single-channel conductance is largely independent of the nature of the membrane lipid [11, 32], in contrast to the behavior of translocatory ion carriers.

A structural model of the gramicidin channel has been proposed by Urry [72, 74]. According to this

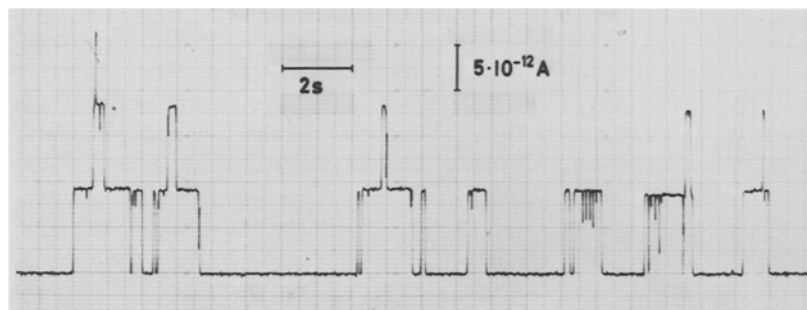


Fig. 3. Conductance fluctuations of a planar bilayer membrane (glycerolmonooleate/*n*-decane) in the presence of very small amounts of gramicidin A. A voltage of 100 mV was applied between the aqueous solutions (1 M CsCl , 25°C). The fluctuations of membrane current arise from the formation and disappearance of single cation-permeable channels. The observed single-channel current corresponds to a flow of $6 \times 10^7 \text{ Cs}^+$ ions per second [8]

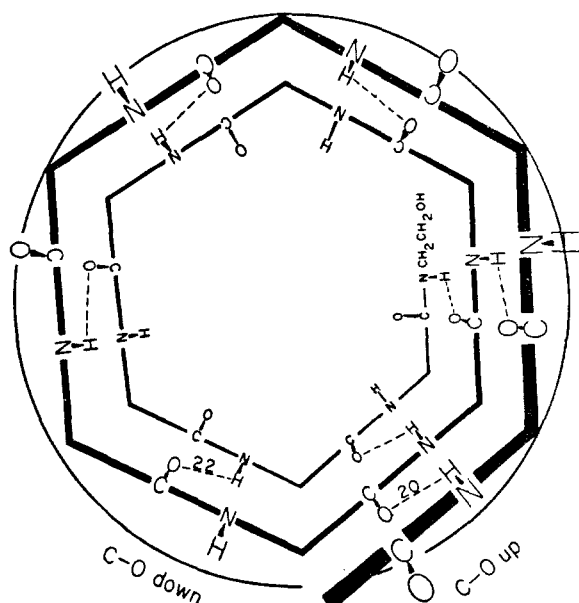


Fig. 4. Structure of the π^6 (L,D)-helix of gramicidin A [74]. The hole along the helix axis has a diameter of 0.4 nm and is lined with oxygen atoms of the peptide carbonyls. Hydrophobic amino-acid residues located at the periphery of the helix are not shown. The transmembrane channel consists of two helices joined at the formyl end

model now supported by many experimental findings [5, 9, 10, 43, 77, 80], the channel consists of a helical dimer that is formed by head-to-head (formyl end to formyl end) association of two gramicidin monomers and is stabilized by intra- and inter-molecular hydrogen bonds (Fig. 4). The central hole along the axis of the π^6 (L,D)-helix has a diameter of about 0.4 nm and is lined with oxygen atoms of the peptide carbonyls, whereas the hydrophobic amino-acid residues lie on the exterior surface of the helix. The total length of the dimer is about 2.5–3.0 nm, the lower limit of the hydrophobic thickness of the lipid bilayer.

The exact mechanism by which ions move through the channel is still a matter of speculation. The entry of the ion into the channel is made energetically favorable by interaction with the peptide carbonyls. In the 0.4-nm wide channel, water molecules can precede and follow the ion through the channel so that probably only part of the primary hydration shell is stripped off. The interaction with the ligand groups creates a series of potential energy minima along the pathway of the ion. Superimposed onto this potential is the dielectric interaction of the ion with the water phase and the membrane lipid which should give rise to a broad energy barrier with the peak in the middle of the membrane [50, 51]. If this picture is correct, then an energetically favorable “binding” site for the ion should exist close to either

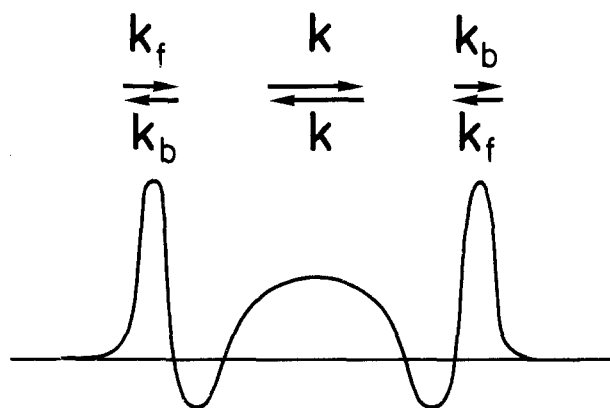


Fig. 5. Hypothetical potential-energy profile of an ion in the gramicidin channel used to analyze single-channel conductance and biionic potential data [33]. Variations of the potential resulting from the geometry of the ligand systems have been omitted. In the analysis of the model it is assumed that an ion can jump from left to right only when the right-hand binding site is empty, and vice versa (single-filing condition). k_f and k_b are the forward and backward rate constants for the binding of the ion to the empty channel. k_f^* and k_b^* are the corresponding rate constants for a channel with the second binding site occupied

end of the channel (Fig. 5). If such a channel is occupied by two ions at the same time, the ions may interact with each other electrostatically. Indeed, several observations, such as concentration-dependent permeability ratios [25, 56], blocking effects of Tl^+ ions [25, 58, 59], the peculiar shape of the conductance-concentration dependence [5, 9–11, 25, 32, 43, 50, 51, 56, 58, 59, 72, 74, 77, 80] and deviations from Ussing’s flux ratio relation [63] support the notion of ion-ion interactions within the channel. These findings have been analyzed on the basis of the model depicted in Fig. 5 [4, 33], which contains five kinetic parameters; the forward and backward rate constants k_f and k_b for the binding of the ion (second binding site empty), the corresponding quantities k_f^* and k_b^* (second binding site occupied), and the rate constant k of translocation across the central barrier. Using the concentration and voltage dependence of single-channel conductance and the permeability ratios and fitting the model to the experimental data, the values of the rate constants given in Table 2 have been obtained [33]. These values predict that the first binding site becomes occupied already at ion concentrations in range of 1–10 mM ($k_b/k_f \approx 8$ mM for Na^+). Another interesting prediction is the large increase in dissociation rate after the second binding site has been occupied ($k_b^*/k_b \approx 600$). Such a result, of course, may be expected from the electric repulsion between the ions; it is unclear, however, why a simi-

Table 2. Rate constants of ion transport through the gramicidin channel, according to the model shown in Fig. 5 [33]^a

	Cs ⁺	K ⁺	Na ⁺	Na ⁺ (NMR)
$k_f/10^8 \text{ M}^{-1} \text{ s}^{-1}$	1.8	1.6	0.55	0.3
$k_b/10^5 \text{ s}^{-1}$	2.9	3.9	4.5	3
$k_f^*/10^8 \text{ M}^{-1} \text{ s}^{-1}$	1.6	1.4	0.53	0.12
$k_b^*/10^8 \text{ s}^{-1}$	1.6	2.1	2.6	0.4
$k/10^7 \text{ s}^{-1}$	8.2	2.7	1.3	>0.03

^a Values in the first three columns have been obtained from single-channel conductance and biionic voltage data [33], values in the last column from NMR studies with ²³Na⁺ in a micellar system [76].

lar effect on the association rates is not seen. The rate constants determined in this way have to be considered as tentative since the analysis is based on a limited set of steady-state experiments (electrical relaxation studies of ion transfer kinetics in the channel have not been done so far). More complicated models with more than two binding sites have also been applied to the analysis of conductance and biionic potential measurements [25, 61].

Recently, NMR techniques have been used in the study of ion transport rates in the gramicidin channel [75, 76]. Gramicidin A was incorporated into lysolecithin micelles in aqueous phase and the chemical shift and line width of the ²³Na resonance was measured. The dependence of longitudinal relaxation rate on Na⁺ concentration indicated the presence of a tight and a weak binding site which were interpreted (on the basis of the two-site model of Fig. 5) in terms of binding to the empty and singly-occupied channel, respectively. From the chemical shift and relaxation data the binding constants $K = k_f/k_b$ and $K^* = k_f^*/k_b^*$, as well as the off-rate constants k_b and k_b^* could be approximated. The notion that in the micellar system gramicidin A assumes a structure that is similar to the functional channel structure in a lipid bilayer is supported by the finding that Tl⁺ and Ag⁺ which block single-channel conductance in the bilayer have an inhibitory effect on Na⁺ binding in the micellar system [75]. It may be seen from Table 2 that the NMR-derived rate constants of Na⁺ transport agree with an order of magnitude with the rate constants obtained from conductance data.

Steady-State Behavior of Carriers and Channels

Steady-state measurements of transport rates as a function of concentration and voltage may be used as a source of information on transport mechanisms. From such studies it is often possible to exclude particular mechanisms, when the observed behavior is at variance with the predictions of the model. What

are the criteria a given transport process has to fulfill in order to be classified as a carrier or a channel mechanism? A general answer to this question is difficult, because different versions of carrier and channel models are feasible and certain models may have rather complicated properties [49]. For instance, a carrier may have more than one binding site and there may be positive or negative cooperativity between the sites. Furthermore, as will be discussed later, intermediate transport systems are feasible that are neither carriers nor channels in the usual sense. Straight-forward criteria, however, may be easily established for "simple" carriers or "simple" channels [22, 45, 52, 53], e.g., channels with fixed barrier structure and single occupancy.

In the following, we shall compare simple channel and carrier models with respect to a number of measurable quantities. The net flux Φ (mol/sec) from left to right of the transported ion will be given as a function of the concentrations c' and c'' and of the membrane voltage $V = \psi' - \psi''$ (ψ is the electric potential; ' and '' denote the left-hand and right-hand side, respectively). The net flux Φ may be written as the difference of two unidirectional fluxes Φ' (left to right) and Φ'' (right to left):

$$\Phi = \Phi' - \Phi'' \quad (1)$$

Furthermore, it is useful to introduce the unidirectional flux Φ_o under equilibrium conditions:

$$\Phi_o \equiv (\Phi')_{c'=c''; V=0} = (\Phi'')_{c'=c''; V=0} \quad (2)$$

In some cases the unidirectional equilibrium flux Φ_o is related in a simple way to the ohmic conductance λ_o of the transport system which is defined by

$$\lambda_o = zF \left(\frac{d\Phi}{dV} \right)_{V=0; c'=c''} \quad (3)$$

z is the valency of the ion and F is Faraday's constant. Φ' and Φ'' can be measured if the transported ion species is present as an isotope pair A, B :

$$\begin{array}{c|c} c'_A & c''_A \quad c'_A + c'_B = c' \\ c'_B & c''_B \quad c''_A + c''_B = c'' \\ \psi' & \psi'' \quad V = \psi' - \psi'' \end{array}$$

Φ' and Φ'' are then defined in the following way:

$$\Phi' = (\Phi_A)_{c'_B=c''_A=0} = \frac{c'}{c'_A} (\Phi_A)_{c'_A=0} \quad (4)$$

$$\Phi'' = -(\Phi_A)_{c''_B=c'_A=0} = -\frac{c''}{c''_A} (\Phi_A)_{c'_A=0} \quad (5)$$

The second part of Eqs. (4) and (5) refers to the usual experimental situation where a small amount of a

“hot” isotope A is added to one side and the flux of this isotope is measured.

If ions move independently through the membrane (for instance by free diffusion at low concentration), the ratio of the unidirectional fluxes obeys Ussing’s relation

$$\frac{\Phi'}{\Phi''} = \frac{c'}{c''} \exp(zu) = \exp[z(u - u_o)]. \quad (6)$$

u is the reduced voltage and u_o the value of u at equilibrium:

$$u \equiv \frac{V}{RT/F} = \frac{\psi' - \psi''}{RT/F}; \quad u_o = \frac{1}{z} \ln \frac{c''}{c'}. \quad (7)$$

For a comparison of different transport systems it is convenient to represent the flux ratio in the form

$$\frac{\Phi'}{\Phi''} = \exp[nz(u - u_o)]; \quad n = \frac{\ln(\Phi'/\Phi'')}{z(u - u_o)}. \quad (8)$$

For systems obeying Ussing’s relation the flux-ratio exponent n is unity. For channels with ion-ion interaction and carriers, n is, in general, a function of voltage and concentrations (see below). From the relation

$$\lambda_o = \frac{zF^2}{RT} \Phi_o \left[\frac{d}{du} \left(\frac{\Phi'}{\Phi''} \right) \right]_{u=0; c'=c''} \quad (9)$$

which follows from Eqs. (1)–(3), it is seen that λ_o , Φ_o and n are connected by [34, 36]:

$$\lambda_o = \frac{z^2 F^2}{RT} \Phi_o \cdot (n)_{u=0; c'=c''}. \quad (10)$$

Transport systems may be further distinguished by their coupling properties. Let A and B be two molecular species that are transported by the same transport system. The fluxes Φ_A and Φ_B are said to be coupled if Φ_A does not only depend on the electrochemical potential difference $\Delta\tilde{\mu}_A$ of species A , but also on $\Delta\tilde{\mu}_B$ (and vice versa). The coupling behavior is most conveniently described in the vicinity of equilibrium, i.e., for small driving forces $\Delta\tilde{\mu}_A$ and $\Delta\tilde{\mu}_B$. Under the condition

$$\begin{aligned} c'_A &= c_A + \Delta c_A; & c''_A &= c_A; & |\Delta c_A| &\ll c_A \\ c'_B &= c_B + \Delta c_B; & c''_B &= c_B; & |\Delta c_B| &\ll c_B \\ |V| &\ll RT/F \end{aligned} \quad (11)$$

the difference in electrochemical potential is given by

$$\Delta\tilde{\mu}_A \approx RT \frac{\Delta c_A}{c_A} + zFV \quad (12)$$

$$\Delta\tilde{\mu}_B \approx RT \frac{\Delta c_B}{c_B} + zFV. \quad (13)$$

R is the gas constant and T the absolute temperature. In the vicinity of equilibrium the fluxes Φ_A and Φ_B are linearly related to the driving forces $\Delta\tilde{\mu}_A$ and $\Delta\tilde{\mu}_B$:

$$\Phi_A = L_A \Delta\tilde{\mu}_A + L_{AB} \Delta\tilde{\mu}_B \quad (14)$$

$$\Phi_B = L_{BA} \Delta\tilde{\mu}_A + L_B \Delta\tilde{\mu}_B. \quad (15)$$

The phenomenological coefficients L_A , L_B , L_{AB} , L_{BA} are functions of concentration. The cross coefficients L_{AB} and L_{BA} which describe the coupling behavior of the transport system obey the relations $L_{AB} = L_{BA}$ and $L_{AB}L_{BA} \leq L_AL_B$ [39]. As we shall see, carriers and channels differ in a characteristic way in the cross coefficients L_{AB} .

Most flux-coupling experiments are carried out under the condition that A and B are isotopically labeled species with identical transport properties. In this case the phenomenological coefficients are related by [62]:

$$L_{AB} = \frac{L_A c_B - L_B c_A}{c_A - c_B}. \quad (16)$$

The total flux $\Phi = \Phi_A + \Phi_B$ of the isotope pair is described by

$$\Phi = L_o \Delta\tilde{\mu} \quad (17)$$

where $L_o = L_A(c_B = 0) = L_B(c_A = 0) > 0$.

Finally we introduce the tracer permeability coefficient $P^* = \Phi_o/c$ and the ordinary permeability coefficient P which is defined by $P = \Phi/\Delta c$ (for $V=0$ and $|\Delta c| \ll c$). These quantities are connected by the important relation [31, 62]:

$$f \equiv \frac{P^*}{P} = 1 - \frac{c^2 L_{AB}}{c_A c_B L_o} = \frac{1}{(n)_{u=0; c'=c''=c}} \quad (18)$$

where f is the so-called correlation factor [28] and $c = c_A + c_B$ is the total concentration of the isotope pair. It is seen from Eq. (18) that (in the vicinity of equilibrium) a flux-ratio exponent n larger than unity is always associated with positive flux coupling ($L_{AB} > 0$)

Channel with Fixed Barrier Structure and Single Occupancy

A channel may be represented by a series of “binding sites” that are separated by energy barriers (Fig. 6). The binding sites are the minima in the potential

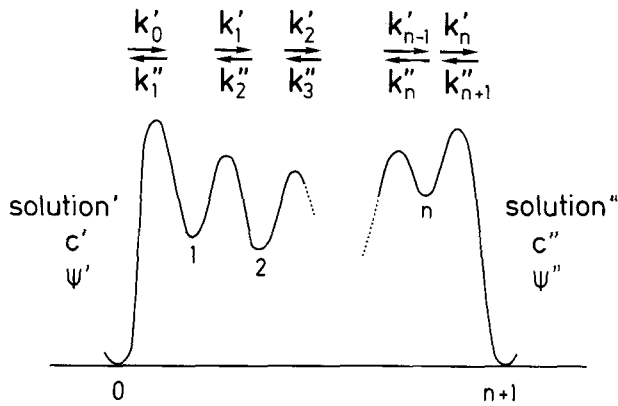


Fig. 6. Potential energy of an ion in the channel. k'_i and k''_i are the rate constants for jumps from i -th energy minimum to the right and to the left, respectively. c' and c'' are the concentrations of the permeable ion species and ψ' and ψ'' are the electrical potentials in the aqueous solutions

energy profile which result from interactions of the ion with one or several ligand groups of the channel. The following discussion is restricted to ion channels with fixed barrier structure, i.e., with an energy profile that is independent of time and independent of the movement of the ion. Furthermore, we assume that an ion can enter the channel only if the channel is empty so that there is no more than one ion in the channel at a time. The frequency of jumps of the ion out of the i -th minimum to the right and to the left is described by rate constants k'_i and k''_i , respectively (Fig. 6). If the permeable ion species is present in concentrations c' and c'' in the left and right aqueous solution, the ion flux through a membrane containing N mol channels is given by [46]:

$$\Phi = N k'_0 v \frac{c' - c'' \exp(-zu)}{1 + \sum_{i=1}^n S_v + v c' Q' + v c'' Q'' \exp(-zu)} \quad (19)$$

$$Q' \equiv \sum_{v=1}^n \sum_{\mu=1}^v S_v R_\mu \quad (20)$$

$$Q'' \equiv \sum_{i=1}^n R_v + \sum_{v=2}^n \sum_{\mu=1}^{v-1} R_v S_\mu \quad (21)$$

$$S_v \equiv \frac{k'_1 k'_2 \dots k'_v}{k''_1 k''_2 \dots k''_v} \quad (22)$$

$$R_v \equiv \frac{k'_0 k'_1 \dots k'_{v-1}}{k''_1 k''_2 \dots k''_v} \quad (23)$$

For $n=1$, Q'' is defined as $Q'' \equiv R_1 = k'_0/k''_1$. The quantity v which has the dimension of a volume is defined by the probability p that the outermost energy minimum on the solution side of the channel mouth is

occupied by an ion:

$$p_0 = v c'; \quad p_{n+1} = v c''. \quad (24)$$

The rate constants for ion translocation depend on voltage. If α_i is the fraction of total voltage $V = \psi' - \psi''$ which drops across the i -th barrier (which is to the left of the i -th binding site) then

$$k'_i = \bar{k}'_i \exp(\alpha_{i+1} z u / 2) \quad (25)$$

$$k''_i = \bar{k}''_i \exp(-\alpha_i z u / 2). \quad (26)$$

\bar{k}'_i and \bar{k}''_i are the values of k'_i and k''_i at zero voltage. According to the principle of microscopic reversibility the rate constants are not independent from each other but are connected by the relation

$$\frac{k'_0 k'_1 \dots k'_n}{k''_1 k''_2 \dots k''_{n+1}} = \exp(z u). \quad (27)$$

The unidirectional fluxes Φ' and Φ'' [Eqs. (3) and (4)] are obtained as [46]:

$$\Phi' = N v c' (1 - p) \frac{k'_0}{1 + \sum_{i=1}^n S_v} \quad (28)$$

$$\Phi'' = N v c'' (1 - p) \frac{k'_0}{1 + \sum_{i=1}^n S_v} \exp(-z u) \quad (29)$$

where p is the probability that the channel is occupied by an ion. It is seen that the unidirectional fluxes do not only depend on the concentration of the *cis* side (c' in the case of Φ') but also (via the concentration dependence of p) on the concentration of the *trans* side. According to Eqs. (28) and (29) the ratio of the unidirectional fluxes is given by

$$\frac{\Phi'}{\Phi''} = \frac{c'}{c''} \exp(z u) \quad (30)$$

which is identical with Ussing's flux-ratio relation ($n=1$). For the channel model considered here, Ussing's relation still holds, although ions compete for the binding sites of the channel.

From Eq. (28) the unidirectional flux Φ_0 under equilibrium conditions [Eq. (2)] is obtained as:

$$\Phi_0 = \frac{N v c}{1 + c K} \cdot \frac{\bar{k}'_0}{1 + \sum_{i=1}^n \bar{S}_v} \quad (31)$$

(Here and in the following quantities referring to the equilibrium state ($c' = c'' = c$, $u = 0$) are marked by a bar). K is the equilibrium constant of ion binding to the channel (i.e., $c K$ is equal to the ratio of occupied

to empty channels) and is given by

$$K = v \sum_1^n \bar{R}_v. \quad (32)$$

From Eq. (19) the ohmic conductance of the channel system is obtained as

$$\lambda_o = \frac{z^2 F^2}{RT} \cdot \frac{N v c}{1 + K c} \cdot \frac{\bar{k}'_o}{1 + \sum_1^n \bar{S}_v}. \quad (33)$$

Comparison with Eq. (31) shows that for the model considered here the simple relation

$$\lambda_o = \frac{z^2 F^2}{RT} \Phi_o \quad (34)$$

holds. (Eq. (34) may also be obtained from Eq. (10) with $n=1$.) According to Eqs. (31) and (33) both Φ_o and λ_o saturate at ionic concentrations $c \gg 1/K$.

In the presence of an isotope pair A, B the fluxes Φ_A and Φ_B are described (in the vicinity of equilibrium) by the phenomenological coefficients $L_A, L_B, L_{AB}=L_{BA}$ [Eqs. (14) and (15)] which are obtained as

$$L_A = \frac{1}{RT} \cdot \frac{v c_A}{1 + (c_A + c_B)K} \cdot \frac{\bar{k}'_o}{1 + \sum_1^n \bar{S}_v} \quad (35)$$

$$L_B = \frac{1}{RT} \cdot \frac{v c_B}{1 + (c_A + c_B)K} \cdot \frac{\bar{k}'_o}{1 + \sum_1^n \bar{S}_v} \quad (36)$$

$$L_{AB}=L_{BA}=0. \quad (37)$$

These equations may be interpreted in the following way. The transport of ion species A and B does not obey the independence principle [35], since the coefficient L_A describing the flux of A does not only contain c_A but also the concentration c_B of the other species. The origin of this nonindependence of ion flows lies in the fact that both ion species compete for the same binding sites in the channel. On the other hand, as shown by Eq. (37), flux coupling does not occur and accordingly the flux ratio equation [Eq. (30)] agrees with Ussing's relation. Eqs. (30) and (37) are no longer obeyed, however, when ions interact within the channel (*see below*).

Carrier with Single Binding Site

We consider a neutral carrier with a single binding site functioning according to the reaction scheme shown in Fig. 2. This scheme, of course, is not

restricted to translatory carriers; the processes described by the rate constants k_S and k_{MS} could also be conformational transitions exposing the binding site alternately to the left and to the right aqueous phase. Furthermore, for generality we assume that the carrier is asymmetric so that, for instance, the association-rate constant k'_R on the left side may be different from the rate constant k''_R on the right side. As all rate constants may depend on voltage, such an asymmetry is created even for an intrinsically symmetric carrier system in the presence of a nonzero membrane potential.

Again, the eight rate constants are not independent of each other, but are connected by the relation

$$\frac{k'_R k'_{MS} k''_D k''_S}{k''_R k''_{MS} k'_D k'_S} = \exp(z u). \quad (38)$$

The net flux Φ and the unidirectional fluxes Φ' and Φ'' through a membrane containing N carrier molecules are given by the following expressions [45, 65]:

$$\Phi = N k'_R k'_{MS} k''_D k''_S \frac{c' - c'' \exp(-z u)}{\alpha + \beta c' + \gamma c'' + \delta c' c''} \quad (39)$$

$$\Phi' = N k'_R k'_{MS} k''_D k''_S \frac{c' + \varepsilon c' c''}{\alpha + \beta c' + \gamma c'' + \delta c' c''} \quad (40)$$

$$\Phi'' = N k'_R k'_{MS} k''_D k''_S \frac{c'' \exp(-z u) + \varepsilon c' c''}{\alpha + \beta c' + \gamma c'' + \delta c' c''} \quad (41)$$

$$\alpha \equiv (k'_S + k''_S)(k'_D k''_D + k'_D k''_{MS} + k'_D k''_{MS}) \quad (42)$$

$$\beta \equiv k'_R [k'_D (k'_{MS} + k''_S) + k'_S (k'_{MS} + k''_{MS})] \quad (43)$$

$$\gamma \equiv k''_R [k'_D (k'_{MS} + k'_S) + k'_S (k'_{MS} + k''_{MS})] \quad (44)$$

$$\delta \equiv k'_R k''_R (k'_{MS} + k''_{MS}) \quad (45)$$

$$\varepsilon \equiv \frac{1}{\alpha} \left(\frac{1}{k'_S} + \frac{1}{k''_S} \right) k'_R k''_{MS} k'_D k'_S. \quad (46)$$

It is seen from Eqs. (39)–(41) that the flux equations for the carrier, which contain terms proportional to $c' c''$, have a more complicated concentration dependence than the corresponding equations for a channel. From Eqs. (40) and (41) the ratio of unidirectional fluxes and the flux-ratio exponent n [Eq. (8)] are obtained as

$$\frac{\Phi'}{\Phi''} = \exp[z(u - u_o)] \cdot \frac{1 + \varepsilon c''}{1 + \varepsilon c'' \exp[z(u - u_o)]} \quad (47)$$

$$n = 1 + \frac{1}{z(u - u_o)} \ln \frac{1 + \varepsilon c''}{1 + \varepsilon c'' \exp[z(u - u_o)]} \leq 1. \quad (48)$$

Equations (47) and (48) express the fact that carriers do not obey Ussing's relation. Flux-ratio exponents

$n \leq 1$ are characteristic for carrier-mediated transport. It is seen from Eq. (47) that under saturation conditions ($\varepsilon c'' \gg 1$, $\varepsilon c'' \exp z(u - u_o) \gg 1$) the flux ratio approaches unity, irrespective of the magnitude of the driving force. From Eqs. (39) and (40) the unidirectional flux Φ_o at equilibrium and the ohmic conductance λ_o are obtained as

$$\Phi_o = N \bar{k}'_R \bar{k}'_{MS} \bar{k}''_D \bar{k}''_S c \frac{1 + \bar{\varepsilon} c}{\bar{\alpha} + (\bar{\beta} + \bar{\gamma}) c + \bar{\delta} c^2} \quad (49)$$

$$\lambda_o = \frac{z^2 F^2}{RT} \cdot \frac{\Phi_o}{1 + \bar{\varepsilon} c}. \quad (50)$$

It is seen from Eq. (50) that in carrier-mediated ion transport Eq. (34) no longer holds and λ_o/Φ_o becomes concentration dependent.

In order to calculate the phenomenological coefficients of Eqs. (14) and (15) we assume, for simplicity, that the carrier is symmetric for $V=0$ ($\bar{k}'_R = \bar{k}''_R \equiv k_R$, etc.) and that the interfacial reactions are always in equilibrium ($c k_R$ and k_D much larger than k_S and k_{MS}). The results then read (with $k_R/k_D = K$):

$$L_A = \eta(k_S + k_{MS} K c_B) c_A \quad (51)$$

$$L_B = \eta(k_S + k_{MS} K c_A) c_B \quad (52)$$

$$L_{AB} = L_{BA} = -\eta k_{MS} K c_A c_B \quad (53)$$

$$\eta = \frac{N k_{MS} K / 2RT}{k_S + K(k_S + k_{MS})(c_A + c_B) + k_{MS} K^2 (c_A + c_B)^2}. \quad (54)$$

Equation (53) shows that (in agreement with Eqs. (18) and (48)) the carrier system has a nonzero, negative cross-coefficient. This means that a flow of A drives a flow of B in the opposite direction (and vice versa). This phenomenon, called "negative flux coupling" or "countertransport", is a characteristic property of simple carrier systems. Its origin may be visualized in the following way. Consider an equilibrium situation with $V=0$, $c'_A = c''_A$, $c'_B = c''_B$ in which both fluxes Φ_A and Φ_B vanish. If now c'_A is increased, more carrier molecules will be in the form AS on the left side so that a flux of AS in the membrane from left to right occurs. But at the same time the number of carriers in the form BS on the same side is diminished (as B is displaced from the carrier by A) which leads a net flow of BS from right to left.

If the back transport of the free carrier is very slow ($k_S \approx 0$), then Eqs. (51)–(53) yield $L_A \approx L_B \approx -L_{AB}$ which means that $\Phi_A \approx -\Phi_B$ (compare Eqs. (14) and (15)). Such transport systems in which the fluxes are completely coupled are sometimes called exchange systems. Exchange flow is observed, for instance, in case of the anion transport system in the membrane of red blood cells [21].

Ion-Ion Interaction in Channels

Much evidence has now accumulated that channels in excitable membranes, such as the potassium channel in squid axon, may accommodate more than one ion at a time [1, 12, 31, 36]. In such multiply-occupied channels ions may interact with each other. Part of the interaction results from the coulombic field around the ions; for instance, in a medium of dielectric constant 20 the electrostatic repulsion energy between two univalent cations 0.5 nm apart is about 6 kT. In this way, dissociation of an ion from the channel may be facilitated if a second ion is present in a neighboring binding site. Another more indirect interaction may occur when binding of an ion results in a reorientation of dipolar groups of the channel molecule, which in turn changes the energy profile for a second ion.

A particular aspect of ion-ion interaction is single-file transport which occurs in narrow channels in which ions cannot pass by each other as they move through the channel [12, 36, 29, 44]. The single-file condition can give rise to pronounced flux coupling, in particular, in channels with many binding sites. Experimental tests of single-file models are not easy because the theoretically derived flux equations usually contain many adjustable parameters; for instance, the transport of a single ion species through a three-site single-file channel is described by 19 independent transition-rate constants. The simplest single-file model is a channel with two binding sites. This model, which has been studied in detail [71], has been used to analyze the ionic permeability of the gramicidin channel [33] (see above).

Some of the characteristic properties of single-file channels may be discussed on the basis of a simple special case, a symmetrical two-site channel (Fig. 5) in which the terminal barriers are rate-limiting ($k \gg k_b, k_b^*, c k_f, c k_f^*$). As before, the forward and backward rate constants for the binding of the ion to the empty channel under the condition $u=0$ are denoted by k_f and k_b ; k_f^* and k_b^* are the corresponding rate constants for a channel with the second binding site occupied. Under these conditions, the following relations are obtained from the general equations of reference 71 (with $K \equiv k_f/k_b$ and $K^* \equiv k_f^*/k_b^*$):

$$\Phi_o = \frac{N}{4} \cdot \frac{c K (2k_b + c k_f^*)}{1 + 2c K + c^2 K K^*} \quad (55)$$

$$\lambda_o = \frac{z^2 F^2}{RT} \Phi_o \frac{2(k_b + c k_f^*)}{2k_b + c k_f^*} \quad (56)$$

$$\frac{\Phi'}{\Phi''} = \exp[z(u - u_o)] \cdot \frac{1 + \theta \exp[z(u - u_o)]}{1 + \theta} \quad (57)$$

$$\theta \equiv \frac{c'' k_f'' k_b^*}{k_b^* + k_b^{*''}} \cdot \frac{2k_f k_b''(k_b^* + k_b^{*''}) + k_f^* k_b^{*''}(c' k_f' + c'' k_f'')}{k_f' k_b''(k_b^* + k_b^{*''})(k_b' + r k_b'') + k_f^* k_b^{*''}(c' k_f' k_b' + c'' k_f'' k_b' r)} \quad (58)$$

(Rate constants for jumps across the left and right barrier are denoted by ' and '', respectively; for $u=0$: $k_f' = k_f'' = k_f$, etc.; $r \equiv k'/k''$ is the ratio of jump rate constants across the central barrier from left to right and from right to left).

Again, the flux ratio deviates from Ussing's relation, but now the exponent n is larger than unity:

$$n = 1 + \frac{1}{z(u-u_o)} \ln \frac{1 + \theta \exp[z(u-u_o)]}{1 + \theta} \geq 1 \quad (59)$$

whereas for a carrier, as shown above, the relation $n \leq 1$ holds. For vanishing voltage, Eq. (57) reduces to

$$\left(\frac{\Phi'}{\Phi''}\right)_{u=0} = \frac{c'}{c''} \cdot \frac{1 + \frac{c'' k_f^*}{2k_b} \cdot \frac{c'}{c''}}{1 + \frac{c'' k_f^*}{2k_b}} \quad (60)$$

Thus, in the limit $c'' k_f^* \gg 2k_b$, the relation $\Phi'/\Phi'' = (c'/c'')^2$ holds ($u=0$). This corresponds to $n=2$ which is the maximum value of the flux-ratio exponent for a two-site channel [28, 33]. For $u=0$ and $c' = c'' = c$, Eq. (59) becomes $n = 2(k_b + c k_f^*)/(2k_b + c k_f^*)$, in agreement with Eqs. (10) and (56).

For the two-site channel with rate-limiting terminal barriers, the cross-coefficient L_{AB} for isotope flow is given by

$$L_{AB} = \frac{N}{4RT} \cdot \frac{k_f^* K c_A c_B}{1 + 2K(c_A + c_B) + K K^*(c_A + c_B)^2} \quad (61)$$

In agreement with Eqs. (18) and (59), L_{AB} is always positive, meaning that the flux of species A tends to drive a flux of B in the same direction.

Summary

Transport systems may be distinguished by their coupling properties, using isotopically labeled permeants. Negative flux coupling ($L_{AB} < 0$) or flux-ratio exponents $n < 1$ are characteristic for a carrier with a single binding site. Positive flux coupling, however, may occur when the carrier has more than one binding site for the transported species. A channel with fixed barrier structure that cannot accommodate more than one ion at a time, although it deviates from the independence principle, does not exhibit flux coupling. Nonzero, positive flux coupling and flux-ratio exponents $n > 1$ are predicted for channels with multiple occupancy and single-filing.

Affinity, Transport Rate, and Specificity

An efficient transport system should combine high transport rates with a high affinity. These two requirements are not easy to fulfill simultaneously, since as soon as the interaction energy between ion and binding site becomes high, the rate of dissociation of the ion from the site will be low. Much has still to be learned on how this compromise between affinity and transport rates is accomplished in biological transport systems.

The performance of an ion carrier or channel in terms of transport rate may be described by specifying the turnover number f which is defined as the limiting ion flux Φ/N per single transport-unit under the condition $V=0$, $c''=0$ and $c' \rightarrow \infty$. For a symmetrical carrier Eq. (39) yields

$$f \equiv \left(\frac{\Phi}{N}\right)_{c''=0; c' \rightarrow \infty} = \left(\frac{1}{k_S} + \frac{1}{k_{MS}} + \frac{2}{k_D}\right)^{-1} \quad (62)$$

The turnover number of a channel with single occupancy is obtained from Eq. (19). The result for the symmetrical two-site channel (Fig. 5) reads:

$$f = \left(\frac{1}{k} + \frac{2}{k_b}\right)^{-1} \quad (63)$$

and for a channel with $(n+1)$ identical barriers:

$$f = \frac{2k_i}{n(n+1)} \quad (64)$$

where k_i is the rate constant of crossing the barrier.

The affinity of the transport system is described by the equilibrium constant K of ion binding, which for the channel is given by $K = k_f/k_b$. A large value of K can ultimately be achieved only if k_b becomes small, since the association rate constant k_f is limited by diffusion of ions towards the binding site. Introduction of $k_b < k_{f, \text{diff}}/K$ into Eq. (63) yields

$$fK < \frac{1}{2} k_{f, \text{diff}} \quad (65)$$

Thus, the product of turnover rate and equilibrium constant of binding can never be larger than the association rate constant $k_{f, \text{diff}}$ in a diffusion-controlled reaction, which is of the order of $10^9 \text{ M}^{-1} \text{ s}^{-1}$. If, for instance, K is 100 M^{-1} (corresponding to a half-saturation concentration of 10 mM), the turnover rate can be at most $5 \times 10^6 \text{ s}^{-1}$. This prediction is consistent with the properties of ion channels studied so far. A completely analogous expression holds for carrier-mediated transport.

The turnover rate of a translocatory carrier of the valinomycin type is mainly limited by the translocation rate constants k_S and k_{MS} [Eq. (62)] which depend on the viscous interaction of the carrier with the lipid. Experimental values of k_S and k_{MS} for valinomycin and similar carriers are of the order of $10^4 - 10^5 \text{ s}^{-1}$ (see above). It is obvious that much higher transport rates may be achieved in a channel. A general distinction between carriers and channels on the basis of transport rates seems difficult, however, since carriers may exist in which the binding site is switched between left- and right-exposed state by minor conformational transitions, and in this case high transport rates are feasible.

An important property of transport systems is the ability to discriminate between chemically similar permeants. If two ion species A and B are considered, the selectivity may be expressed by the ratio χ of the tracer permeability coefficients in the limit of low ion concentration:

$$\chi \equiv \left(\frac{P_A^*}{P_B^*} \right)_{c_A, c_B \rightarrow 0}. \quad (66)$$

For the symmetrical two-site channel (Fig. 5) the selectivity ratio χ is obtained as (using Eq. (31) together with $P^* = \Phi_0/c$):

$$\chi = \frac{K_A}{K_B} \cdot \frac{k_A(1 + 2k_B/k_b^B)}{k_B(1 + 2k_A/k_b^B)} \quad (67)$$

($K = k_f/k_b$). The corresponding expression for the symmetrical carrier reads

$$\chi = \frac{K_A}{K_B} \cdot \frac{k_{MS}^A(1 + 2k_{MS}^B/k_D^B)}{k_{MS}^B(1 + 2k_{MS}^A/k_D^A)}. \quad (68)$$

($K = k_R/k_D$). It is seen from Eqs. (67) and (68) that the selectivity ratio is the product of a "thermodynamic" term (containing equilibrium binding constants) and of a "kinetic" term (containing rate constants). This means that selectivity cannot be understood on the basis of equilibrium binding properties alone [6]. If binding becomes very strong (k_b small and k_f close to the diffusion limit) then Eq. (67) reduces to

$$\chi \simeq \frac{k_f^A}{k_f^B} \quad (k_b \ll k). \quad (69)$$

In this case selectivity becomes small, since ions of comparable size should have very similar values of $k_{f, \text{diff}}$.

In the case of a translocatory carrier the translocation rate constant k_{MS} should not depend much on the nature of the complexed ion; if, in addition, the condition $k_D \gg k_{MS}$ is fulfilled for both ion species, Eq.

(68) reduces to

$$\chi \simeq \frac{K_A}{K_B} \quad (k_D \gg k_{MS}; k_{MS}^A \approx k_{MS}^B). \quad (70)$$

The range of conditions under which Eq. (70) holds has been termed "equilibrium domain" of the transport mechanism [24]. The molecular basis of ion selectivity of equilibrium binding, which is probably more or less the same for carriers and channels, has been discussed in considerable detail in terms of ion-ligand interactions [23, 30, 73].

It is obvious that a transport system, in order to be highly selective, must interact strongly with the permeants. This in turn requires a compromise between selectivity and transport rate. High ion transport rates have been observed, for instance, with membrane pores formed by the matrix protein of *Escherichia coli* in artificial bilayer membranes; these 1-nm wide, probably water-filled pores barely discriminate between small ions [16, 17]. At the other extreme are transport systems that distinguish sharply between structurally similar compounds, such as D-glucose and L-glucose; in this case the observed transport rates are low. Highly specific transport is often considered as indicative of a carrier mechanism. This criterium should be applied with caution, however, since rather specific interactions between permeant and ligand system may occur in a channel, too [57]. The general prediction seems to be justified, however, that highly specific transport systems tend to be slow, irrespective of the particular permeation mechanism.

Channels with Multiple Conformational States: A Unifying Concept

As discussed above, ion transport in a channel may be described as a series of thermally activated processes in which the ion moves from a binding site across an energy barrier to an adjacent site. In this treatment the energy levels of wells and barriers are usually considered to be fixed, i.e., independent of time and not influenced by the movement of the ion. This description, which corresponds to an essentially static picture of protein structure, represents a useful approximation in certain cases. Recent findings on the dynamics of protein molecules, however, suggest the use of a more general concept of barrier structure.

A protein molecule in thermal equilibrium may exist in a large number of conformational states and may rapidly move from one state to the other [26, 54]. Evidence for fluctuations of protein structure comes from X-ray diffraction studies [26, 37],

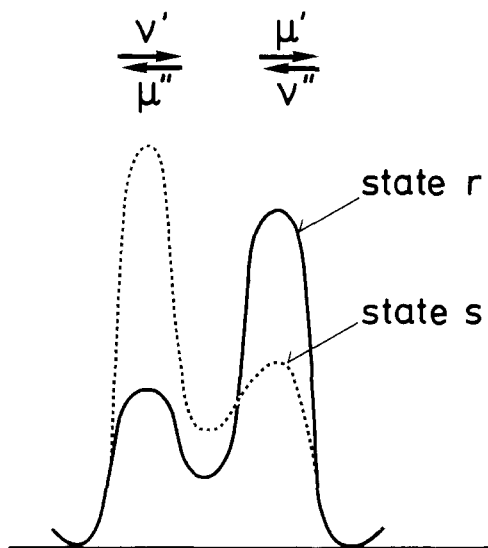


Fig. 7. Energy profile of a channel with two conformational states. The rate constants for the transfer of the ion between binding site and aqueous phase are v'_r , v'_s , μ'_r , μ'_s (state r) and v''_s , v''_r , μ''_s , μ''_r (state s)

NMR [78], and optical [55] experiments and from the kinetic analysis of ligand rebinding to myoglobin after flash photolysis [7]. These and other studies have shown that internal motions in proteins occur in the time range from picoseconds to seconds. This suggests that the energy profile of a channel (Fig. 6) is subjected to fluctuations over a wide spectrum of times.

Of particular interest is the possibility that transitions between conformational states of the channel protein may be coupled to the movement of the ion within the channel [27]. Such a coupling may result, for instance, from electrostatic interactions between ion and ligand system. When an ion jumps into a binding site, the strong coulombic field around the ion tends to polarize the neighborhood by reorienting dipolar groups of the protein. This reorientation is likely to shift the energy level of the binding site and the height of adjacent barriers. If the rate of conformational change induced by the ion is comparable to or smaller than the jump rate, the ion may leave the binding site before the protein structure has relaxed to the polarized state. Likewise, after the ion has left a binding site, a certain time is required for the channel to return to the original conformation, and the next ion may find the structure still in a partly polarized state [2, 79]. Changing the ion concentration in the aqueous phase (and thus the average occupancy of the channel) may shift the distribution of conformational states of the channel and affect its permeability. As will be shown below, this behavior can lead to a nonlinear concentration dependence of permeability different from the simple saturation

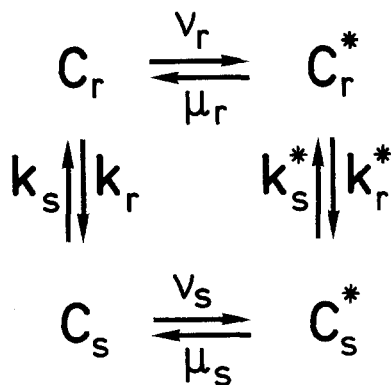


Fig. 8. Transitions between the four substrates of a channel with one binding site (C_r : conformation r , empty; C_r^* : conformation r , occupied; C_s : conformation s , empty; C_s^* : conformation s , occupied)

characteristics predicted for channels with fixed barrier structure and single occupancy.

It is obvious that a channel with variable energy profile is intermediate between a carrier and a channel with fixed barrier structure and includes the carrier mechanism as a limiting case. If a channel has in one state a low barrier at the left mouth and a high barrier at the right mouth whereas in another state the left-hand barrier is high and the right-hand barrier low, then transitions between these two conformations correspond to the switching of a binding side from a left- to a right-exposed state, a characteristic feature of carrier function.

Two-State Channel with Single Binding Site

A general treatment of multistate channels is, of course, rather complicated; in the following we discuss the simple case of a two-state channel with a single binding-site (Fig. 7), which already exhibits some of the basic properties of channels with variable barrier structure [48]. It is assumed that the channel molecule may exist in four distinct substrates:

- C_r : conformation r , empty;
- C_r^* : conformation r , occupied;
- C_s : conformation s , empty;
- C_s^* : conformation s , occupied.

The rate constants for transitions between these substrates are indicated in Fig. 8. Transitions between empty and occupied states may occur by exchange of an ion between the binding site and the left or right aqueous phase. Thus (Fig. 7):

$$v_r = v'_r + v''_r = c' \rho'_r + c'' \rho''_r \quad (71)$$

$$v_s = v'_s + v''_s = c' \rho'_s + c'' \rho''_s \quad (72)$$

$$\mu_r = \mu'_r + \mu''_r \quad (73)$$

$$\mu_s = \mu'_s + \mu''_s. \quad (74)$$

The jump rates v'_r , v''_r , v'_s , v''_s of ions into the empty side are assumed to be proportional to aqueous ion concentration (c' , c''), whereas μ'_r , μ''_r , μ'_s , μ''_s are true monomolecular rate constants.

The principle of microscopic reversibility requires that the rate constants obey the following relation [48]:

$$\frac{v'_r \mu'_r}{v''_r \mu''_r} = \frac{v'_s \mu'_s}{v''_s \mu''_s} = \frac{v'_r \mu'_s k_s^*}{v''_r \mu''_s k_r^*} = \exp[z(u - u_0)]. \quad (75)$$

The ion flux Φ is obtained as [48]:

$$\Phi = \frac{N}{\sigma} \{1 - \exp[-z(u - u_0)]\} \cdot [v'_r \mu'_r (v_s k_s^* + k_s k_s^* + \mu_s k_s) + v'_s \mu'_s (v_r k_r^* + k_r k_r^* + \mu_r k_r) + v'_r \mu'_s k_s k_r^* + v'_s \mu'_r k_r k_s^*] \quad (76)$$

$$\sigma \equiv (k_r + k_s)(\mu_r \mu_s + \mu_r k_s^* + \mu_s k_r^*) + (k_r^* + k_s^*)(v_r v_s + v_r k_s + v_s k_r) + v_r \mu_s (k_s + k_r^*) + v_s \mu_r (k_r + k_s^*). \quad (77)$$

This gives for the mean single-channel conductance A the expression ($c' = c'' = c$; $\rho'_r + \rho''_r = \rho_r$; $\rho'_s + \rho''_s = \rho_s$; L is Avogadro's constant):

$$A(c) = \frac{\lambda_o}{N} = \frac{z^2 F^2}{RTL} \cdot \frac{c(A + Bc)}{C + Dc + Ec^2} \quad (78)$$

$$A \equiv \rho'_r \mu'_r k_s (\mu_s + k_s^*) + \rho'_s \mu'_s k_r (\mu_r + k_r^*) + \rho'_r \mu'_s k_s k_r^* + \rho'_s \mu'_r k_r k_s^* \quad (79)$$

$$B \equiv \rho'_r \rho_s \mu'_r k_s^* + \rho'_s \rho_r \mu'_s k_r^* \quad (80)$$

$$C \equiv (k_r + k_s)(\mu_r \mu_s + \mu_r k_s^* + \mu_s k_r^*) \quad (81)$$

$$D \equiv (k_r^* + k_s^*)(\rho_r k_s + \rho_s k_r) + \rho_r \mu_s (k_s + k_r^*) + \rho_s \mu_r (k_r + k_s^*) \quad (82)$$

$$E \equiv \rho_r \rho_s (k_r^* + k_s^*). \quad (83)$$

(According to the definition of λ_o , the rate constants refer to voltage $u=0$ in these equations). It is seen from Eq. (78) that $A(c)$ is a nonlinear function of ion concentration containing terms which are quadratic

in c . This behavior may be compared with the properties of a one-site channel with fixed barrier structure which, according to Eq. (33) always exhibits a simple saturation characteristic of the form

$$A(c) = \frac{\lambda_o}{N} = \frac{z^2 F^2}{RT} \cdot \frac{\rho c}{\mu + \rho c} \cdot \frac{\mu' \mu''}{\mu} \quad (84)$$

(Eq. (84) is obtained from Eq. (33) by the substitutions $n=1$, $v c \bar{k}'_o = v'$, $\bar{k}'_1 = \mu'$, $\bar{k}''_1 = \mu''$; $c(v' + v'') = \rho$).

It can easily be shown that for certain combinations of rate constants $A(c)$ goes through a maximum with increasing ion concentration. Such a non-linear concentration dependence of conductance is usually taken as evidence for ion-ion interaction in the channel or for the existence of regulatory binding sites. In the channel model discussed here the non-linearity of $A(c)$ is connected with the fact that the distribution of channel molecules between states r and s depends on ion concentration and that both states have, in general, different (concentration-dependent) conductances.

For the further discussion of Eq. (78) it is useful to consider two limiting cases in which conformational transitions are either much slower or much faster than ion-translocation.

Case 1: $k_r, k_s, k_r^*, k_s^* \ll v_r, v_s, \mu_r, \mu_s$.

Under this condition the mean lifetime of a given state is much longer than the time an ion spends in the energy well. Equation (78) then reduces to

$$A = p_r A_r + (1 - p_r) A_s \quad (85)$$

where A_r and A_s are the conductances of the channel in states r and s , respectively, which have the form of Eq. (84). p_r is the probability of finding the channel in state r (under equilibrium conditions) and is given by (with $K_r \equiv v_r/\mu_r$, $K_s \equiv v_s/\mu_s$, $\kappa \equiv k_r/k_s$, $\kappa^* \equiv k_r^*/k_s^*$, $\theta \equiv k_s^*/k_s$):

$$p_r = \frac{(1 + c K_r)(1 + c K_s \theta)}{(1 + c K_r)(1 + c K_s \theta) + (1 + c K_s)(\kappa + c K_r \theta \kappa^*)}. \quad (86)$$

Thus, when the transition rates are small, A becomes equal to the weighted average of the conductances in states r and s . In this case many ions enter and leave the channel during the life-time of the individual state. (When the mean life-times of the two states become sufficiently long, transitions between r and s may be directly observed in a single-channel experiment.) Since p_r depends on ion concentration, a non-linear concentration dependence of A results which is different from the simple saturation behavior [Eq. (84)] of A_r and A_s .

Case 2: $k_r, k_s, k_r^*, k_s^* \gg v_r, v_s, \mu_r, \mu_s$.

When interconversion of states r and s is much faster than ion transfer between binding site and water, states r and s are always in equilibrium with each other, even for nonzero ion flow through the channel. This equilibrium may be described by introducing the probability a_r that an empty channel is in state r and the probability a_r^* that an occupied channel is in state r :

$$a_r = \frac{1}{1 + \kappa}; \quad a_r^* = \frac{1}{1 + \kappa^*}. \quad (87)$$

Under the condition of fast conformational transitions, Eq. (78) reduces to the simple form of Eq. (84) when the following substitutions are introduced:

$$\rho = a_r \rho_r + (1 - a_r) \rho_s \quad (88)$$

$$\mu' = a_r^* \mu'_r + (1 - a_r^*) \mu'_s \quad (89)$$

$$\mu'' = a_r^* \mu''_r + (1 - a_r^*) \mu''_s. \quad (90)$$

This means that in the limit of fast interconversion the equation for A becomes formally identical to the corresponding equation derived for a channel with fixed barrier structure, provided that the rate constants are replaced by weighted averages of the rate constants in the two states. This result (which can be generalized to multi-site channels with more than two conformational states [48]) had to be expected since under the above conditions the lifetime of a given conformation is much shorter than the time an ion spends in the binding site and therefore the ion "sees" an average barrier structure. Despite the formal identity of the conductance equation with Eq. (84), the interpretation of the transport process in a channel with variable barrier structure is different, since an ion will preferably jump over the barrier when the barrier is low; this means that the jump rate largely depends on the frequency with which conformational states with low barrier heights are assumed.

The Carrier Mechanism as a Limiting Case

When in one state the barrier to the right is very high (binding site mainly accessible from the left) and in the other state the barrier to the left (binding site mainly accessible from the right), then the transport model approaches a carrier mechanism. Indeed, in the limit $\mu'_r \approx 0$, $\rho'_r \approx 0$, $\mu'_s \approx 0$, $\rho'_s \approx 0$, Eq. (76) transforms into Eq. (39) for carrier-mediated ion flux when the following substitutions are introduced: $\rho'_r = k'_R$, $\mu'_r = k'_D$, $\rho'_s = k''_R$, $\mu'_s = k''_D$, $k_r = k'_S$, $k_s = k''_S$, $k_r^* = k'_{MS}$, k_s^*

$= k''_{MS}$. The idea that carrier operation may involve conformational transitions switching a binding site from a left-exposed to a right-exposed state has extensively been discussed in the literature [38, 42, 49, 60]; experimental evidence for the existence of conformational states differing in the orientation of the binding site has been obtained in the case of the ATP/ADP exchange system in mitochondria [42].

Ion Pumps

The concept of channels with multiple conformational states may also be applied to ion pumps. An ion channel functions as a pump when the energy profile of the channel is transiently modified in an appropriate way by an energy-supplying reaction [38, 47, 60]. Absorption of a light-quantum, transition to another redox state, or phosphorylation of the channel protein may alter the binding constant of an ion-binding site in the channel and, at the same time, change the height of adjacent barriers. In this way an ion may be preferentially released to one side of the membrane, while during the transition back to the original state of the channel another ion is taken up from the opposite side.

As a specific example we consider the light-driven proton pump in the purple membrane of halobacteria [69]. A minimum model [47, 68] of the pumping cycle is depicted in Fig. 9. It is assumed that in the ground state (HP) of the pump a proton is located in a binding site which is accessible from the left (cytoplasmic) phase but separated from the right (external) phase by a high barrier. Absorption of a photon creates an activated state HP^* (via short-lived intermediates) in which the energy level of the binding site is shifted upward (corresponding to a decrease of binding strength). In the activated state the barrier heights are changed in such a way that the proton is released preferentially to the right (external) solution. After dissociation of the proton, the channel molecule relaxes back to a conformation with a low barrier on the left (cytoplasmic) side ($P^* \rightarrow P$). The original state is restored by uptake of H^+ from the cytoplasmic side ($P \rightarrow HP$). The whole cycle is equivalent to a net transfer of a proton from the cytoplasm (phase') to the external medium (phase'').

The rate constant p for transitions from the ground state to the excited state depends on light intensity J :

$$p = p_o + \gamma J. \quad (91)$$

p_o is the rate constant of spontaneous transitions $HP \rightarrow HP^*$ in the dark, and γ is the absorption cross

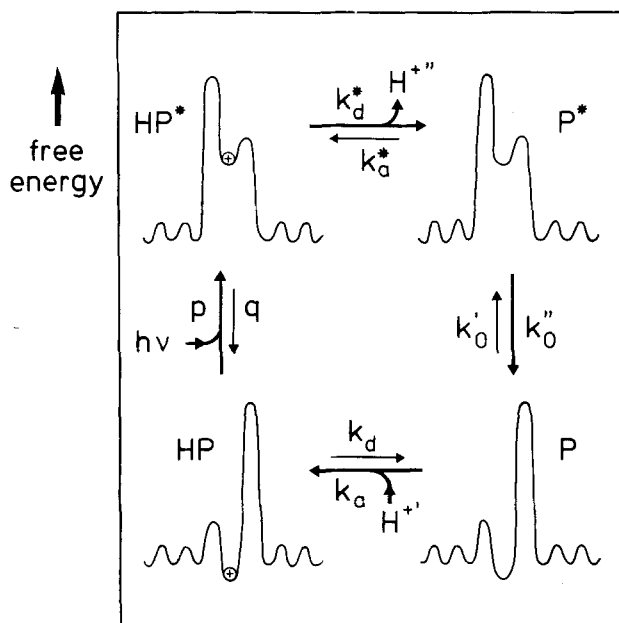


Fig. 9. Channel mechanism for a light-driven proton pump. The energy profile of the channel is transiently modified by absorption of a photon. In the ground state HP the proton binding site is exposed to the left-hand aqueous phase (phase') and in excited state HP^* to the right-hand phase (phase''). During the decay of the excited state back to the ground state (via P^* and P) a proton is released to phase'' and another proton is taken up from phase'

section. If the pump starts to work at zero initial voltage ($V \equiv \psi' - \psi'' = 0$) and equal proton activities in both aqueous phases ($a' = a''$), a difference in the electrochemical potential $\tilde{\mu}_H$ of H^+ builds up, which consists partly of a voltage V and partly of a pH difference. With increasing $\Delta\tilde{\mu}_H$ the rates of the reverse processes ($P^* + H^{+''} \rightarrow HP^*$, $HP \rightarrow P + H^{+'}$) are enhanced so that eventually a limiting value of $\Delta\tilde{\mu}_H$ is reached at which the net rate of proton transfer vanishes. In the absence of leakage pathways this limiting value is given by [47]:

$$(\Delta\tilde{\mu}_H)_{\max} = - \left(RT \ln \frac{a'}{a''} + FV \right)_{\max} \\ = RT \ln \frac{p_o + \gamma J}{p_o + \gamma J \exp(-h\nu/kT)} \quad (92)$$

$(\Delta\tilde{\mu}_H)_{\max}/F$ is the so-called proton-motive force of the pump. As the photon energy $h\nu$ is much higher than the thermal energy kT , the term $\gamma J \exp(-h\nu/kT)$ in the denominator can often be neglected. On the other hand, it is seen from Eq. (92) that $(\Delta\tilde{\mu}_H)_{\max}$ can never exceed the value $Lh\nu$ ($L=R/k$ is Avogadro's constant).

The maximum turnover rate f of the pump may be defined as the proton flux (referred to a single pump molecule), observed under the condition $a' = a''$

$= a$, $V=0$, $J \rightarrow \infty$. Using the rate constants as indicated in Fig. 9, f is obtained as [47]:

$$f = \left[\frac{1}{k_d^*} + \frac{1}{k_o''} + \frac{1}{a k_a} + \frac{k_o'}{k_o'' k_d} \left(1 + \frac{a}{K^*} \right) \frac{K}{a} + \frac{a}{K^*} \frac{1}{k_o''} \right]^{-1} \quad (93)$$

$K \equiv k_d/k_a$ and $K^* \equiv k_d^*/k_a^*$ are the proton dissociation constants in the ground state and excited state, respectively.

It is interesting to note that the expression for $(\Delta\tilde{\mu}_H)_{\max}$ [Eq. (92)] does not contain the proton dissociation constants K and K^* . This means that a pK difference between ground state and excited state is not a necessary condition for a large proton-motive force. The essential feature of the pumping mechanism is a light-induced change of barrier structure which switches the proton binding site from a left-exposed to a right-exposed state. On the other hand, as seen from Eq. (93), a low pH of the excited state ($K^* \gg a$) and a high pK of the ground state ($K \ll a$) is favorable for a high turnover rate of the pump. In fact, the highest rate is achieved when the dark reactions become virtually irreversible ($a k_a^* \approx 0$, $k_o' \approx 0$, $k_d \approx 0$):

$$f = \left(\frac{1}{k_d^*} + \frac{1}{k_o''} + \frac{1}{a k_a} \right)^{-1} \quad (94)$$

Conclusion

A unified description of ion carriers, channels, and pumps seems possible based on the concept of channels with multiple conformational states. The notion of a channel with variable energy profile is suggested by recent work on the dynamics of proteins. With the exception of mobile, translocatory carriers of the valinomycin type which represent a separate class of ion translocators, most transport systems in biological membranes seem to be built-in proteins. Transmembrane proteins may differ in their mode of operation by the extent to which conformational changes are involved in the translocation of the permeant. While carriers and channels in the usual sense are limiting cases of a multistate channel, many real transport systems probably function by an intermediate mechanism.

References

1. Aityan, S.K., Kalandadze, I.L., Chizmadjev, Y.A. 1977. *Bioelectrochem. Bioenerg.* 4:30
2. Andersen, O.S. 1975. U. Lassen and J.O. Wieth, editors. P. 369. 5th International Biophysics Congress, Copenhagen (*Abstr.*)

3. Andersen, O.S., Fuchs, M. 1975. *Biophys. J.* **15**:795
4. Andersen, O.S., Procopio, J. 1980. *Acta Physiol. Scand.* **481** (Suppl.):27
5. Apell, H.-J., Bamberg, E., Alpes, H., Läuger, P. 1977. *J. Membrane Biol.* **31**:171
6. Armstrong, C.M. 1975. *Q. Rev. Biophys.* **7**:179
7. Austin, R.M., Beeson, K.W., Eisenstein, L., Frauenfelder, H., Gunsalus, I.C. 1975. *Biochemistry* **14**:5355
8. Bamberg, E., Alpes, H., Apell, H.-J., Benz, R., Janko, K., Kolb, H.-A., Läuger, P., Gross, E. 1977. In: *Biochemistry of Membrane Transport*, FEBS-Symposium No. 12. G. Semenza and E. Carafoli, editors. pp. 179–201. Springer, Berlin
9. Bamberg, E., Apell, H.-J., Alpes, H. 1977. *Proc. Nat. Acad. Sci. USA* **74**:2402
10. Bamberg, E., Läuger, P. 1973. *J. Membrane Biol.* **11**:177
11. Bamberg, E., Noda, K., Gross, E., Läuger, P. 1976. *Biochim. Biophys. Acta* **419**:223
12. Begenisich, T., DeWeer, P. 1977. *Nature (London)* **269**:710
13. Benz, R., 1978. *J. Membrane Biol.* **43**:367
14. Benz, R., Cros, D. 1978. *Biochim. Biophys. Acta* **506**:265
15. Benz, R., Fröhlich, O., Läuger, P. 1977. *Biochim. Biophys. Acta* **46**:465
16. Benz, R., Janko, K., Boos, W., Läuger, P. 1978. *Biochim. Biophys. Acta* **511**:305
17. Benz, R., Janko, K., Läuger, P. 1979. *Biochim. Biophys. Acta* **551**:238
18. Benz, R., Läuger, P. 1976. *J. Membrane Biol.* **27**:171
19. Benz, R., Stark, G., Janko, K., Läuger, P. 1973. *J. Membrane Biol.* **14**:339
20. Burgermeister, W., Winkler-Oswatitsch, R. 1977. *Top. Curr. Chem.* **69**:91
21. Cabantchik, Z.I., Knauf, P.A., Rothstein, A. 1978. *Biochim. Biophys. Acta* **515**:239
22. Devés, R., Krupka, R.M. 1979. *Biochim. Biophys. Acta* **556**:533
23. Eisenman, G. 1969. In: *Ion-Selective Electrodes*. R.A. Durst, editor. pp. 1–56. National Bureau of Standards Special Publication 314. U.S. Government Printing Office, Washington
24. Eisenman, G., Krasne, S., Ciani, S. 1975. *Ann. N.Y. Acad. Sci.* **264**:34
25. Eisenman, G., Sandblom, J., Neher, E. 1978. *Biophys. J.* **22**:307
26. Frauenfelder, H., Petsko, G.A., Tsernoglou, D. 1979. *Nature (London)* **280**:558
27. Frehland, E. 1979. *Biophys. Struct. Mechan.* **5**:91
28. Heckmann, K. 1965. *Zs. Physik. Chem. NF* **46**:1
29. Heckmann, K. 1972. In: *Biomembranes*. F. Kreuzer and J.F.G. Slegers, editors. Vol. 3, p. 127. Plenum Press, New York
30. Hille, B. 1975. In: *Membranes — A Series of Advances*. G. Eisenman, editor. pp. 255–323. M. Dekker, New York
31. Hille, B., Schwarz, W. 1978. *J. Gen. Physiol.* **72**:409
32. Hladky, S.B., Haydon, D.A. 1972. *Biochim. Biophys. Acta* **274**:294
33. Hladky, S.B., Urban, B.W., Haydon, D.A. 1979. In: *Membrane Transport Processes*. C.F. Stevens and R.W. Tsien editor. Vol. 3, pp. 89–103. Raven Press, New York
34. Hodgkin, A.L. 1951. *Biol. Rev.* **26**:339
35. Hodgkin, A.L., Huxley, A.F. 1952. *J. Physiol. (London)* **116**:449
36. Hodgkin, A.L., Keynes, R.D. 1955. *J. Physiol. (London)* **128**:61
37. Huber, R., Deisenhofer, J., Colman, P.M., Matshushima, M., Palm, W. 1976. *Nature (London)* **264**:415
38. Jardetzky, O. 1966. *Nature (London)* **211**:969
39. Katchalsky, A., Curran, P.F. 1967. *Nonequilibrium Thermodynamics in Biophysics*. Chapter 8. Harvard University Press, Cambridge (Mass.)
40. Kauzmann, W. 1957. *Quantum Chemistry*. Chapter 16. Academic Press, New York
41. Ketterer, B., Neumcke, B., Läuger, P. 1971. *J. Membrane Biol.* **5**:225
42. Klingenberg, M., Riccio, P., Aquila, H., Buchanan, B.B., Grebe, 1976. In: *The Structural Basis of Membrane Function*. Y. Hatefi and L. Djavadi-Ohanian, editors. pp. 293–311. Academic Press, New York
43. Koeppe, R.E., II, Hodgson, K.O., Stryer, L. 1978. *J. Mol. Biol.* **121**:41
44. Kohler, H.-H. 1977. *Biophys. J.* **19**:125
45. Kotyk, A., Janáček, K. 1977. In: *Biomembranes*. L.A. Manson, editor. Vol. 9, Sect. 4.3. Plenum Press, New York
46. Läuger, P. 1973. *Biochim. Biophys. Acta* **311**:423
47. Läuger, P. 1979. *Biochim. Biophys. Acta* **553**:143
48. Läuger, P., Stephan, W., Frehland, E. 1980. *Biochim. Biophys. Acta (in press)*
49. LeFevre, P.G. 1975. *Curr. Top. Membr. Transp.* **7**:109
50. Levitt, D.G. 1978. *Biophys. J.* **22**:209
51. Levitt, D.G. 1978. *Biophys. J.* **22**:221
52. Lieb, W.R., Stein, W.D. 1974. *Biochim. Biophys. Acta* **373**:165
53. Lieb, W.R., Stein, W.D. 1974. *Biochim. Biophys. Acta* **373**:178
54. McCammon, J.A., Wolynes, P.G., Karplus, M. 1979. *Biochemistry* **18**:927
55. Munro, I., Pecht, I., Stryer, L. 1979. *Proc. Nat. Acad. Sci. USA* **76**:56
56. Myers, V.B., Haydon, D.A. 1972. *Biochim. Biophys. Acta* **274**:313
57. Naftalin, R.J. 1970. *Biochim. Biophys. Acta* **211**:65
58. Neher, E. 1975. *Biochim. Biophys. Acta* **401**:540
59. Neher, E., Sandblom, J., Eisenman, G. 1978. *J. Membrane Biol.* **40**:97
60. Patlak, C.S. 1957. *Bull. Math. Biophys.* **19**:209
61. Sandblom, J., Eisenman, G., Neher, E. 1977. *J. Membrane Biol.* **31**:383
62. Sauer, F. 1978. In: *Membrane Transport in Biology*. G. Giebisch, D.C. Tosteson and H.H. Ussing, editors. Vol. I, pp. 140–168. Springer-Verlag, Berlin
63. Schagina, L.V., Grinfeldt, A.E., Lev, A.A. 1978. *Nature (London)* **273**:243
64. Shemyakin, M.M., Ovchinnikov, Yu.A., Ivanov, V.T., Antonov, V.K., Vinogradova, E.I., Shkrob, A.M., Malenkov, G.G., Estratov, A.V., Laine, I.A., Melnik, E.I., Ryabova, I.D. 1969. *J. Membrane Biol.* **1**:402
65. Stark, G. 1973. *Biochim. Biophys. Acta* **298**:323
66. Stark, G., Benz, R. 1971. *J. Membrane Biol.* **5**:133
67. Stark, G., Ketterer, B., Benz, R., Läuger, P. 1971. *Biophys. J.* **11**:981
68. Stoekenius, W. 1979. In: *Membrane Transduction Mechanisms*. Cone and Dowling, editors. Raven Press, New York
69. Stoekenius, W., Lozier, R.M., Bogomolni, R.A. 1979. *Biochim. Biophys. Acta* **505**:215
70. Szabo, G., Eisenman, G., Laprade, R., Ciani, S.M., Krasne, S. 1973. In: *Membranes — A Series of Advances*. G. Eisenman, editor. Vol. II, pp. 179–328. M. Dekker, New York
71. Urban, B.W., Hladky, S.B. 1979. *Biochim. Biophys. Acta* **554**:410
72. Urry, D.W. 1971. *Proc. Nat. Acad. Sci. USA* **68**:672
73. Urry, D.W. 1978. *Ann. N. Y. Acad. Sci.* **307**:3
74. Urry, D.W., Goodall, M.C., Glickson, J.D., Mayers, D.F. 1971. *Proc. Nat. Acad. Sci. USA* **68**:1907
75. Urry, D.W., Venkatachalam, C.M., Spisni, A., Bradley, R.J., Trapane, T.L., Prasad, K.U. 1980. *J. Membrane Biol.* **55**:29
76. Urry, D.W., Venkatachalam, C.M., Spisni, A., Läuger, P., Khaled, M. A. 1980. *Proc. Nat. Acad. Sci. USA* **77**:2028
77. Veatch, W.R., Stryer, L. 1977. *J. Mol. Biol.* **113**:89
78. Wagner, G., Wüthrich, K. 1978. *Nature (London)* **275**:247
79. Weber, G. 1965. In: *Molecular Biophysics*. B. Pullman and M. Weissbluth, editors. pp. 369–396. Academic Press, New York
80. Weinstein, S., Wallace, B.A., Blout, E.R., Morrow, J.S., Veatch, W. 1979. *Proc. Nat. Acad. Sci. USA* **76**:4230